Metals **2014**, *4*, 1-7; doi:10.3390/met4010001

OPEN ACCESS

metals

ISSN 2075-4701

www.mdpi.com/journal/metals/

Article

A Concept for the Control of Pore Size in Superalloy Membranes

Joachim Rösler *, Waldemar Krause and Björn Hinze

Institut für Werkstoffe, Technische Universität Braunschweig, Langer Kamp 8, D-38106 Braunschweig, Germany; E-Mails: waldemar.krause2@freenet.de (W.K.); b.hinze@tu-bs.de (B.H.)

* Author to whom correspondence should be addressed; E-Mail: j.roesler@tu-bs.de; Tel.: +49-531-391-3061; Fax: +49-531-391-3058.

Received: 29 November 2013; in revised form: 19 December 2013 / Accepted: 23 December 2013 / Published: 9 January 2014

Abstract: A new method to adjust the pore size in superalloy membranes is shown, utilizing controlled cooling from solution heat treatment of the solid superalloy. Hereby, the nucleation rate and, thus, the size of the γ'-precipitates can be varied to a large extent. This leads to a corresponding variation in the pore size once the membrane material is produced by directional coarsening of the γ'-phase to an interconnected network and subsequent selective extraction of the γ-phase. Furthermore, it was found that coherent and incoherent γ'-precipitates can be used alike to fabricate superalloy membranes, and yet, result in vastly different pore morphologies. The findings widen the application range of this novel material class.

Keywords: superalloys; porous materials; nanostructured materials; heat treatment

---

1. Introduction

Porous metals exhibiting open porosity are of interest for many functional applications, such as filtration or noise attenuation [1,2]. These materials are mainly produced by sintering of powders or fibers [3], coating of polymer sponges [4] or melt infiltration techniques [5]. Resulting pore sizes of these "conventional" porous metals are typically in a range between 10 μm and 100 μm. An alternative manufacturing process was introduced in 2003 [6]. In contrast to the previously mentioned processes, a solid material, namely a Ni-based superalloy is used. It typically contains 50%–70% γ'-precipitates with dimensions of some hundred nanometers in the solution and precipitation heat treated state. Their

shape is cubic with the cube faces oriented perpendicular to crystallographic <001> orientations. When the material is exposed to elevated temperatures, say 1000 °C, the precipitates grow preferentially in specific <001> directions due to external or internal stresses, often referred to as directional coarsening or rafting (see e.g., [7–9]). Eventually, the γ'-particles connect to a network embedded in the γ-matrix, which itself remains continuous. Thus, a microstructure results where the γ- and γ'-phases form two interpenetrating networks. When sheets of such material are produced and one phase is selectively extracted by an (electro-)chemical process, the other phase remains as a self-supporting structure so that a membrane material with open porosity results [6,10–12]. The obtained pore shape is highly elongated as a consequence of the directional coarsening process and the width of these channel-like pores is of the order of some hundred nanometers, *i.e.*, more than an order of magnitude smaller than the pore size achievable in conventional porous metals. Considering this, it is apparent that superalloy membranes widen the range of achievable pore sizes to significantly smaller dimensions. However, it is also apparent that there is currently a gap between the pore size of superalloy membranes and the smallest pore size achievable in conventional porous metals. In order to close this gap, it would be highly beneficial if superalloy membranes, with larger pores well in the micrometer range, could be produced. One approach explored in [12] to achieve this objective is to increase temperature T and/or duration t of the heat treatment during which directional coarsening occurs. However, this approach has limitations: Firstly, coarsening of the very fine initial γ/γ'-microstructure by diffusion is a slow process in superalloys. Secondly, there are upper bounds for t, due to practical considerations, and T, because ultimately the γ'-volume fraction becomes too small for this phase to connect to a 3-dimensional network. Therefore, an alternative concept is explored here, using the cooling rate from the solutioning temperature as key parameter to control the precipitation kinetics of the γ'-phase and, hence, its initial size.

2. Experimental Details

The material investigated here is the single crystalline Ni-based superalloy CMSX-4® [13]. As reference state we use a heat treatment procedure for the production of porous membranes essentially established in [12]. It encompasses solution heat treatment at 1550 K/2 h, 1561 K/3 h, 1569 K/3 h, 1577 K/2 h, 1586 K/2 h, 1589 K/2 h, 1591 K/2 h, 1594 K/2 h followed by air cooling (AC), precipitation heat treatment at 1353 K/4 h/AC and directional coarsening of the microstructure at 1353 K/1000 h. The microstructure in the solution and precipitation heat treated state is depicted in Figure 1a. After directional coarsening, the material was cut by spark erosion to sheets about 2 mm thick and ground to a final thickness of 280 µm to 370 µm to completely remove the surface layer affected by the erosion process. The γ-matrix was then electrochemically extracted using a potential of 1.3 V and an aqueous electrolyte containing 1% ammonium sulfate and 1% citric acid [12,14]. As a result, a membrane material is obtained, consisting of the γ'-phase and pores at the location of the removed γ-phase (Figure 2a). Note that the dendritic microstructure of cast superalloys cannot be homogenized completely [9]. Thus, there are microstructural differences between dendritic and interdendritic regions. Throughout this paper we show images obtained in the secondary dendrite arms to ensure comparability. Furthermore, the normal of all microstructural images, *i.e.*, the normal of the

sheets, is oriented in casting direction, which is essentially parallel to the [001] orientation of the single crystal.

Figure 1. Microstructure in the solution and precipitation heat treated state, as a function of the cooling rate from solution heat treatment (**a**) air cooling (**b**) 4 K/min (**c**) 1 K/min (**d**) 0.2 K/min [14].

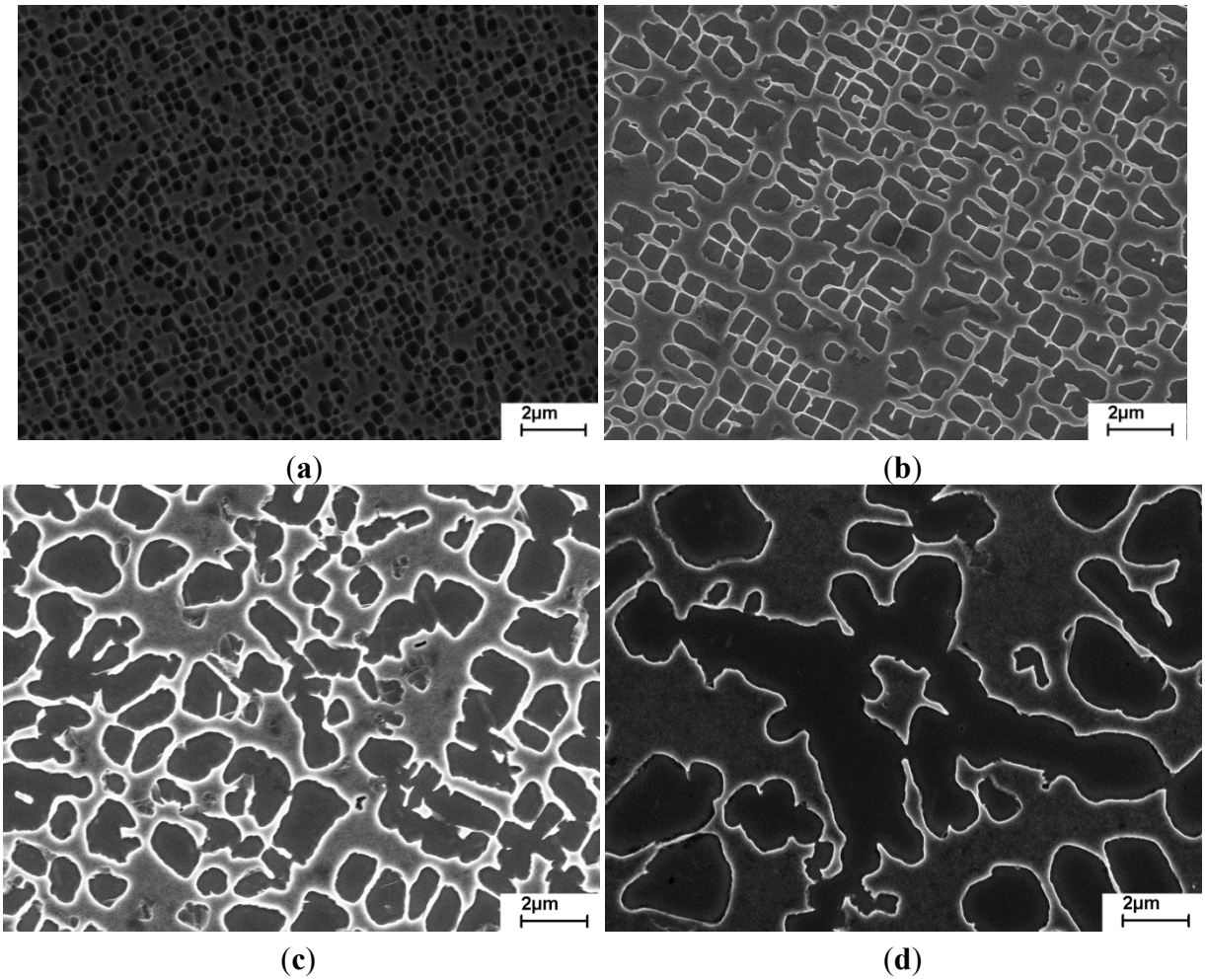

In further experiments, we keep all parameters constant, except for the cooling rate from solution heat treatment. Instead of air cooling, slower cooling at 4 K/min, 1 K/min and 0.2 K/min is selected. Furthermore, cooling from 1594 K is stopped at the precipitation heat treatment temperature of 1353 K followed by a 4 h hold time and air cooling, so that solution and precipitation heat treatment are combined in one cycle. The resulting microstructures after the entire heat treatment cycles are shown in Figure 1b–d. The γ'-particles are significantly larger compared to the reference state and a trend of increasing particle size with decreasing cooling rate is clearly visible. This finding can be understood as follows. It is known, that the precipitation kinetics of γ'-particles in superalloys is very fast [15], so that nuclei are already forming during cooling from the solutioning temperature for all practical purposes. The nucleation rate is strongly dependent on the supercooling below the solvus temperature of the γ'-phase. Fast cooling leads to strong supercooling and, thus, to a high nucleation rate. However, there is little time for particle growth. Consequently, a high density of very fine γ'-particles results. These particles grow during subsequent precipitation heat treatment and the particle density decreases

correspondingly. Yet, the particles are still quite small as illustrated in Figure 1a, which is a consequence of the very fine initial microstructure and the fact that particle ripening by diffusion is a slow process in Ni-based superalloys. When the cooling rate from the solutioning temperature is decreased, there is more time for nucleation to occur. Consequently, the amount of supercooling and, thus, the nucleation rate diminishes. Once a particle is formed, it starts to deplete the surround matrix in the γ'-forming elements (*i.e.*, Al, Ti and Ta), thus hampering nucleation in its vicinity. Both effects lead to a lower particle density. At the same time, the particles become bigger because there is more time for growth during cooling and less competition with neighboring particles for the γ'-forming elements. Consequently, the particle size after solution heat treatment increases with decreasing cooling rate and so does the size after precipitation heat treatment (Figure 1).

Figure 2. Microstructure of the superalloy membranes as a function of the cooling rate from solution heat treatment (**a**) air cooling (**b**) 4 K/min (**c**) 1 K/min (**d**) 0.2 K/min [14].

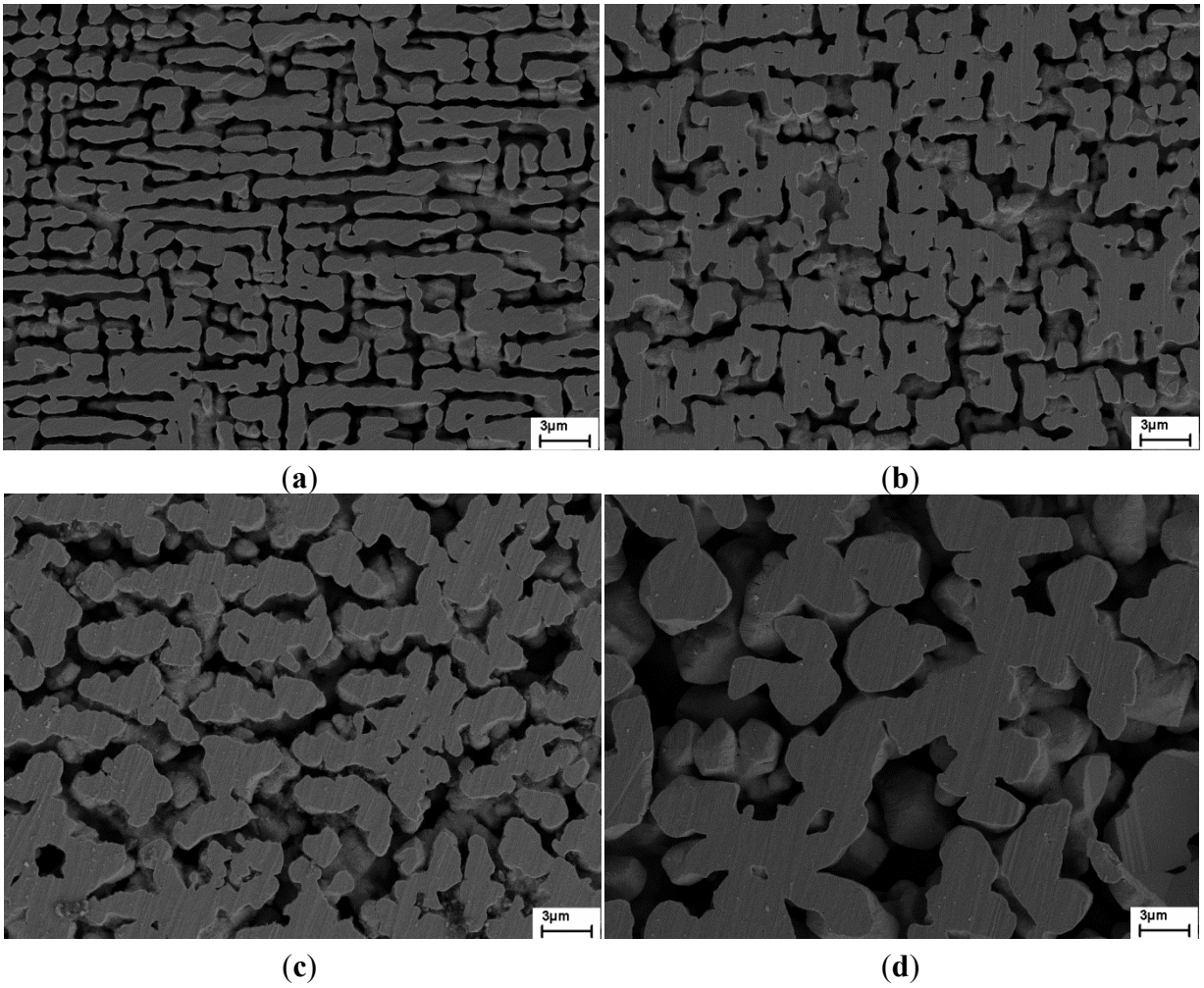

(**a**) (**b**)

(**c**) (**d**)

Besides the size, also the morphology of the γ'-particles is changing with the cooling rate. After air cooling, the particles are cube-shaped (Figure 1a) which minimizes the elastic strain energy associated with the coherent precipitates. When the particles become larger coherency is eventually lost. Then, it is no longer favorable to maintain a cubic shape and the particles become irregular. Such a change in morphology is evident in Figure 1a–d and we deduce from this observation that the particles shown in

Figure 1d are incoherent. In this context, it is important to note that coherency is a prerequisite for directional coarsening to occur. Only then is an interaction between coherency stresses and other stress fields possible, so that the cubic symmetry is lost and particle growth along certain <001>-orientations becomes more favorable. Prior to this study it was unclear whether incoherent particles would also connect to a network as coherent particles do during extended high temperature exposure. To answer this question, all materials were given the same elevated temperature exposure, *i.e.*, 1355 K/1000 h, after solution and precipitation heat treatment. After extraction of the γ-phase, solid membranes were obtained in all cases. It demonstrates that the γ'-particles have connected to a network structure, even in case of incoherency. However, there is a vast difference in the microstructure of the porous membranes (see Figure 2). While directional growth along <001>-directions is evident in Figure 2a,b, the microstructure is entirely irregular in Figure 2d, which can be attributed to the incoherency of the γ'-particles. Although the mechanical behavior of these membranes will be discussed elsewhere, it is worth mentioning that all membranes reached an ultimate tensile strength of at least 10 MPa. This again demonstrates that not only coherent but also incoherent γ'-particles connect to a rigid network upon extended elevated temperature exposure.

Qualitatively, it is apparent from Figure 2 that the pore size is significantly increasing as the cooling rate from the solutioning temperature is decreasing. This result is further quantified in Figure 3, using a line intersection method. Hereby, a set of parallel lines is superimposed on the microstructure image and rotated between 0° and 179° by steps of 1°. The arithmetic average of the lengths in the γ' ligaments and pores is then calculated for every angle and plotted on a polar coordinate system, see [11,12] for further details.

Figure 3 clearly shows an increasing size of the pores and ligaments with decreasing cooling rate. For the pores, 790 ± 109 nm, 928 ± 12 nm, 1167 ± 11 nm and 1928 ± 43 nm are obtained as mean intersect lengths b_{pore} and standard deviations in case of air cooling, and the cooling rates 4 K/min, 1 K/min, 0.2 K/min, respectively. This parameter is defined as the arithmetic average of the intersect lengths obtained for each angle. Note, that there is also a distinct difference in the shape of the curves. In the air cooled reference state, an elliptical shape results. This is due to the preferred orientation of the channel like porosity parallel to a specific {001} plane (Figure 2a). Consequently, the intersect length is longest and shortest parallel and perpendicular to that plane. In contrast, an essentially circular shape is obtained in the other three cases. Even though a cooling rate of 4 K/min still leads to directional porosity, it appears that now all orientations along {001} planes occur about equally (Figure 2b), so that differences in pore length and thickness are not detected by the line intersection method. For the lowest cooling rates of 1 K/min and 0.2 K/min the circular shape simply reflects the irregular morphology of the pores.

Note, that the slowest cooling rate investigated here just adds about 19 h of heat treatment time compared to air cooling. This is sufficient to increase the pore size substantially. In contrast, it is apparent from the data in [12] that a similar extension of the hold time at 1355 K would have no measurable effect on the pore size. This demonstrates the effectivity of the approach explored here and it stands to reason that controlled cooling from the solutioning temperature can be further exploited via even lower cooling rates.

Figure 3. Microstructure ellipses obtained on the superalloy membranes for ligaments and pores as a function of the cooling rate from solution heat treatment.

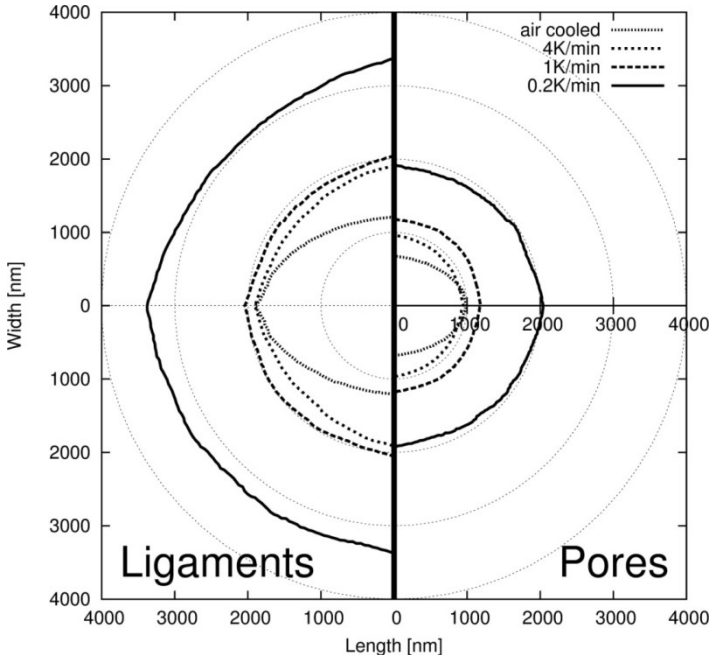

3. Summary and Conclusions

It has been demonstrated that the pore size in superalloy membranes can be effectively controlled via the cooling rate from solution heat treatment, providing a path for the development of superalloy membranes with significantly larger pores than presently possible. This not only allows closing the gap between the pore dimensions of conventional materials with open porosity and current superalloy membranes, it also broadens the application range of superalloy membranes. This in itself is attractive due to specific advantages of these novel materials, such as the ability to form structured sheets consisting of solid and porous domains [16]. Furthermore, it was found that both coherent and incoherent γ'-particles connect to a network upon extended elevated temperature exposure, yet, leading to substantially different morphologies.

Acknowledgments

Financial support of the Deutsche Forschungsgemeinschaft in the frame of the SFB 880 “Grundlagen des Hochauftriebs künftiger Verkehrsflugzeuge” is greatly appreciated.

Conflicts of Interest

The authors declare no conflict of interest.

References

1. Lefebvre, L.-P.; Banhart, J.; Dunand, D.C. Porous metals and metallic foams: Current status and recent developments. *Adv. Eng. Mater.* **2008**, *10*, 775–778.
2. Hinze, B.; Rösler, J.; Lippitz, N. Noise reduction of cellular metals. *Metals* **2012**, *2*, 195–201.

3. Golosnoy, I.O.; Tan, J.C.; Clyne, T.W. Ferrous fibre network materials for noise reduction in gas turbine aeroengines. Part I: Acoustic effects. *Adv. Eng. Mater.* **2008**, *10*, 192–200.
4. Pickering, S. Inco invests in its nickel future at Clydach. *Metal Powder Rep.* **1998**, *53*, 24–27.
5. Brothers, A.H.; Scheunemann, R.; DeFouw, J.D.; Dunand, D.C. Processing and structure of open-celled amorphous metal foams. *Scr. Mater.* **2005**, *52*, 335–339.
6. Rösler, J.; Mukherji, D. Design of nanoporous superalloy membranes for functional applications. *Adv. Eng. Mater.* **2003**, *5*, 916–918.
7. Tien, J.K.; Copley, S.M. The effect of uniaxial stress on the periodic morphology of coherent gamma prime precipitates in nickel-base superalloy crystals. *Metall. Trans.* **1971**, *2*, 215–219.
8. Pollock, T.M.; Argon, A.S. Directional coarsening in nickel-base single crystals with high volume fractions of coherent precipitates. *Acta Metall. Mater.* **1994**, *42*, 1859–1874.
9. Epishin, A.; Link, T.; Brückner, U.; Fedelich, B.; Portella, P. Effects of Segregation in Nickel-Base Superalloys: Dendritic Stresses. In *Superalloys 2004*; Green, K.A., Pollock, T.M., Harada, H., Howson, T.E., Reed, R.C., Schirra, J.J., Walston, S., Eds.; TMS: Warrendale, PA, USA, 2004; pp. 537–543.
10. Rösler, J.; Näth, O.; Jäger, S.; Mukherji, D. Fabrication of nanoporous Ni-based superalloy membranes. *Acta Mater.* **2005**, *53*, 1397–1406.
11. Rösler, J.; Näth, O. Mechanical behavior of nanoporous superalloy membranes. *Acta Mater.* **2010**, *58*, 1815–1828.
12. Hinze, B.; Rösler, J.; Schmitz, F. Production of nanoporous superalloy memmbranes by load-free coarsening of γ'-precipitates. *Acta Mater.* **2011**, *59*, 3049–3060.
13. Harris, K.; Erickson, G.L.; Sikkenga, S.L.; Brentnall, W.D.; Aurrecoechea, J.M.; Kurbarych, K.G. Development of the Rhenium Containing Superalloys CMSX-4® & CM 186 LC® for Single Crystal Blade and Directionally Solidified Vane Applications in Advanced Turbine Engines. In *Superalloys 1992*; Antolovich, S.D., Stusrud, R.W., Mackay, R.A., Anton, D.L., Khan, T., Kissinger, R.D., Klarstrom, D.L., Eds.; TMS: Warrendale, PA, USA, 1992; pp. 297–306.
14. Krause, W. CMSX-4 Gefügeoptimierung für die Membranherstellung. Master Thesis, Technische Universität Braunschweig, Braunschweig, Germany, 2013.
15. Durand-Charre, M. *The Microstructure of Superalloys*; Gordon and Breach Science Publishers: Amsterdam, The Netherlands, 1997.
16. Näth, O.; Stephen, A.; Rösler, J.; Vollertsen, F. Structuring of nanoporous nickel-based superalloy membranes via laser etching. *J. Mater. Process. Technol.* **2009**, *209*, 4739–4743.